

Received July 27, 2020; reviewed; accepted August 30, 2020

## Magnetic field effects on surfactants adsorption on the solid surface as regards of its wettability

Lucyna Hołysz, Emil Chibowski, Konrad Terpiłowski

Institute of Chemical Sciences, Faculty of Chemistry, Department of Interfacial Phenomena, Maria Curie-Skłodowska University in Lublin, 20-031 Lublin, Poland

Corresponding author: [lucyna.holysz@umcs.pl](mailto:lucyna.holysz@umcs.pl) (Lucyna Hołysz)

**Abstract:** The static magnetic field MF (0.44 T) effects on the adsorption of three surfactants: cationic bromide (DTAB) and hexadecyltrimethylammonium bromide (CTAB), and anionic sodium dodecylsulfate (SDS) from their  $10^{-3}$  M solutions were studied on bare and low-temperature air plasma treated glass plates. The surface properties of the adsorbed surfactants layers were determined via the water advancing and receding contact angles measurements and then calculation of the apparent surface free energy. An optical profilometer was used to determine the structure and topography of the adsorbed layers. The DTAB and SDS concentrations were below their critical micelle concentration and that of CTAB very close to its cmc. The results showed that in the case of DTAB solution (much below its cmc) a small decrease in the contact angle appeared while in CTAB (close to its cmc) an increase in the contact angle value was observed if adsorbed in the MF presence. Quite good reproducibility of the contact angle values was obtained. This was not the case for the SDS solution where the contact angle values were scattered. The reason was that the anionic surfactant did not adsorb homogeneously on the negatively charged glass surface. The contact angles and the calculated values of the work of water spreading clearly show that MF influences the structure of the surfactant adsorbed layer which was also supported by the optical profilometry images.

**Keywords:** surfactants, glass surface, magnetic field, adsorption, hydrophobization

### 1. Introduction

Nowadays it is hard to imagine our life without synthetic surfactants in both everyday life and industry. Adsorption of surfactants and their mixtures at the liquid-gas, liquid-liquid and solid-liquid interfaces can change their interfacial properties significantly, therefore they find many practical applications such as in mineral and petroleum processing, biological systems, health and personal care products, foods, crop protection, corrosion inhibition and others (Schramm et al., 2003; Paria and Khilar, 2004; Zhang and Somasundaran, 2006) as well as scientific challenges such as spreading reversal to retraction (Tadmor et al., 2019; Tadmor et al., 2020; Tadmor et al., 2021). One of the important applications of surfactants are enriching processes of the mineral ore and among them the flotation process where the used surfactants are called 'collectors'. Moreover, some other surfactants have to be used as the frothers (Fuerstenau et al., 1964; Leja, 1982; Drzymała, 2007]. It is well known that the role of a collector is to adsorb selectively on the useful mineral (rock) grains to change the surface to sufficiently hydrophobic one, so that they would attach to the gas bubbles which transport them up to the surface where they are collected in the froth. In the minerals processing the froth flotation method is a still widely applied technique for separating particles possessing different chemical and physical characteristics (Drzymała, 1994; Drelich, 2001; Fuerstenau and Somasundaran, 2003; Sadowski and Polowczyk, 2004; Fuerstenau et al. 2007; Bastrzyk et al., 2008; Szymańska and Sadowski, 2010; Didyk and Sadowski, 2012; Gao et al., 2015; Kowalczyk, 2015; Kowalczyk et al., 2016; Kowalczyk, et al. 2017; Drzymała et al., 2016; Drelich, 2018; Gao et al., 2015; Liu, et al. 2019). The the process is thermodynamically described by the Dupre's equation (Adamson and Gast, 1997):

particle/water  $\leftrightarrow$  water/gas  $\rightarrow$  particle/gas

$$\begin{aligned} \gamma_{sg} + \gamma_{lg} &\rightarrow \gamma_{sg} \\ \Delta G &= \gamma_{sg} - (\gamma_{lg} + \gamma_{sl}) \end{aligned} \quad (1)$$

where  $\Delta G$  is the Gibbs' free energy accompanying a gas bubble attachment in water to the hydrophobic particle,  $\gamma_{sg}$  is the solid surface free energy,  $\gamma_{lg}$  is the liquid surface free energy (surface tension), and  $\gamma_{sl}$  is the solid/liquid interfacial free energy. The spontaneous attachment of the particle to a gas bubble occurs at negative  $\Delta G$  (Laskowski, 1989). Because the solid/liquid interfacial free energy is defined as (Zhang, 2013):

$$\gamma_{sl} = \gamma_s + \gamma_l - W_A \quad (2)$$

hence:

$$\Delta G = W_A - 2\gamma_l = W_A - W_C = W_S \quad (3)$$

where  $W_A$  is the work of adhesion of a liquid (water) to a solid surface,  $W_C$  is the work of liquid cohesion and  $W_S$  is the work of liquid spreading.

For clarity in Eq. (2) the subscript **g** at the symbol  $\gamma$  of solid and liquid surface free energy has been omitted. Equation (3) shows that the adhesion of a gas bubble to a solid grain is possible if the work of liquid (water) cohesion  $W_C$  (145.6 mJ/m<sup>2</sup> at 20°C) is greater than the work of liquid adhesion  $W_A$  to the solid surface. This indicates that  $W_S$  must be negative (Chibowski and Holysz, 2006; Rudolf and Hartman, 2017). Along with direct methods [Tadmor et al., 2017], the work of adhesion  $W_A$  can be estimated via the measurement of the liquid (water) contact angle  $\theta$  on the solid (mineral) smooth surface. This results from the Young-Dupre's equation:

$$\gamma_s = \gamma_l \cos\theta + \gamma_{sl} = \gamma_l \cos\theta + \gamma_s + \gamma_l - W_A \quad (4)$$

$$W_A = \gamma_l(1 + \cos\theta) \quad (5)$$

and because the work of spreading  $W_S = W_A - W_C = W_A - 2\gamma_l$ , therefore:

$$W_S = \gamma_l(\cos\theta - 1) = \Delta G \quad (6)$$

The work of adhesion and work of spreading result from the interfacial solid/liquid interactions which can be described in different ways, depending on the theoretical approach (Owens and Wendt 1969; van Oss, et al., 1988). However, as it can be seen from the above, to determine the work of adhesion and work of spreading it is sufficient to measure only the contact angle. The surfactant adsorption changes the solid (mineral) surface from hydrophilic to hydrophobic, which results in an increase of the contact angle (Drelich, 2001).

The adsorption of anionic and cationic surfactants on different solid surfaces was investigated and described in numerous publications (Fan et al., 1997; Atkin et al. 2003; Paria and Khilar, 2004; Koopal et al., 2004; Zhang and Somasundaran, 2006; Li and Ishiguro, 2016; Khan, et al., 2019; Aleksandrova et al., 2020). The studies allowed for elaboration of the adsorption mechanisms and structure of the adsorbed layer of the surfactants (Gaudin and Fuerstenau, 1955; Somasundaran and Fuerstenau, 1966; Harwell et al., 1985; Yeskie and Harwell, 1988; Gao et al., 1987; Gu and Huang, 1989; Rupperecht and Gu, 1991; Cases and Villieras, 1992; Goloub et al. 1996; Goloub and Koopal, 1997; Atkin, et al., 2003; Paria and Khilar, 2004; Golub and Koopal, 2004; Ishiguro and Koopal, 2011).

Somasundran and Fuerstenau (1996) proposed the reverse orientation or four-region model for interpretation of the adsorption isotherm (plotted log-log scales) of anionic surfactant (SDS) on alumina, which also described well the adsorption of this surfactant on rutile (Böhmer and Koopal, 1992a; Böhmer and Koopal, 1992b). They proposed the mechanism of the surfactant layer formation for each of the four distinct regions occurring on the isotherm. According to the four-region model in region I the monomers of surfactant adsorb electrostatically on the oxide surface. Both the polar head and the hydrocarbon chain of the surfactant can interact with the adsorbent surface. In region II, the surfactant adsorption increases and associations of the molecules form hemimicelles. The molecules are oriented with their polar head towards the surface and their hydrophobic chain turned towards the solution. In region III, changes in the structure of surface micelles and formation of bilayer domains takes place. In region IV, the oxide surface is completely covered with the surfactant possessing a structure of bilayer and in the solution the surfactant excess occurs in the form of free micelles (Somasundaran and Fuerstenau, 1966).

Harwell et al. (Harwell et al., 1985; Yeskie and Harwell, 1988) proposed the bilayer model of surfactant adsorption on the heterogeneous solid surface. They assumed that no hemimicelles are formed on the surface below the CMC and above it patches of the surfactant molecules form called admicelles.

According to the Gu et al. model (Gao et al., 1987; Gu and Huang, 1989; Rupprecht and Gu, 1991) the adsorption of surfactant ions on an oppositely charged polar hydrated surface occurs by a two-step mechanism in which the adsorption of surfactant ions is limited by the number of ions initially adsorbed electrostatically. These molecules are the adsorption centres on which small micelles are formed as a result of hydrophobic interactions of alkyl chains. The average number of these surface micelles is fewer than that in the bulk solution. They assumed that small aggregates are of spherical shape which allows for a minimal contact area between the water and the hydrophobic parts of the surfactant ions.

As it results from the above, surfactants adsorption on solid surfaces has been extensively studied and verified experimentally *in situ* by fluorescence studies, electron spin resonance (ESR), vibrational sum-frequency (SFS) and total internal reflection Raman scattering (TIR Raman spectroscopy), AFM (Somasundaran and Huang, 2000; Liu et al., 2001; Tyrode et al., 2008; Karlsson et al., 2010; Hamon et al., 2015; Sokolov et al., 2016; Yi et al., 2018).

However, as to our knowledge, a possible effect of plasma treatment of a solid surface prior to the surfactant adsorption or a static magnetic field treatment effects were not much studied. Therefore, we were interested to know whether these two treatments would influence the surfactant adsorption or properties of the adsorbed layer. For this purpose, the microscope glass as a model surface and three surfactants, i.e. cationic dodecyltrimethylammonium bromide (DTAB) and hexadecyltrimethyl-ammonium bromide (CTAB), and anionic sodium dodecylsulfate (SDS) were used. The critical micellization concentration at 20°C for these surfactants is:  $1.4 \cdot 10^{-2}$  M (Tedeschi, 2003; Bahri et al., 2006),  $0.94 \cdot 10^{-3}$  M (Velegol, 2000), and  $8.4 \cdot 10^{-3}$  M (Zdziennicka et al., 2012), respectively. The glass surface was treated with a low-temperature air plasma before the surfactants adsorption, or, the adsorption from  $10^{-3}$  M solution on the surface occurred in the presence of static magnetic field (ca. 0.44 T). For the comparison, the non-treated glass surface was also investigated. After the surfactant adsorption and drying the surface, the advancing and receding contact angles of water were measured. Then the surface free energy was calculated. Also, the optical profilometry images of the all studied surfaces were obtained.

## 2. Materials and methods

### 2.1. Chemicals and materials

Dodecyltrimethylammonium bromide ( $C_{15}H_{34}BrN$ ) and heksadecyltrimethyl-ammonium bromide ( $C_{19}H_{42}BrN$ ) were purchased from Sigma. Sodium dodecyl sulfate ( $C_{12}H_{25}SO_4$ ) was received from Fluka. The all surfactants ( $\geq 99\%$  pure) were used without further purification. Water from the Milli-Q Plus system was used to prepare  $10^{-3}$ M aqueous solutions a day before their use. The glass microscope plates were purchased from Chemland (Poland).

### 2.2. Glass plates preparation

The adsorption experiments were performed on glass plates ( $3.8 \times 2.6$  cm<sup>2</sup> size) which were obtained by cutting the microscope plates. Next, the plates were cleaned in acetone, then in water using an ultrasonic bath and dried for 30 min at 100°C. The glass plates were stored in a desiccator.

### 2.3. Low-temperature air plasma treatment of glass plates

Plasma treatment of the glass plates was performed in a low pressure plasma system Pico from Diener Electronic, Germany. The glass plates were placed in the vacuum chamber and the system was subjected to a pressure of 0.2 mbar and the gas flow 22 sccm (standard cubic centimeters per minute). The plasma was generated for 60 s at 400 V. In order to remove the gaseous products from the chamber it was purged with air for 10 s, then opened if the inside pressure has increased to the atmospheric one.

### 2.4. Adsorption procedure

The adsorption of DTAB, CTAB or SDS was conducted in the Petri dishes both on the non-treated glass plates and treated with the air plasma. For this purpose, the plate was placed in the dish on two glass

rods and 40 mL of  $10^{-3}$  M surfactant solution was poured in. The adsorption time at  $20 \pm 1^\circ\text{C}$  was 60 min. A similar adsorption tests were carried out in a magnetic field (MF) by placing the Petri dish with the glass plate on a neodymium magnetic stack as shown in Fig. 1A and B. The magnetic field strength was measured using Gaussmeter Model GM-2 (AlphaLab. Inc., USA). On the top of the stack (Fig. 1A) there was the field gradient from 0.51 T (the outer wall) to only 0.08 T in the stack middle. However, along the outer wall of the magnetic stack (Fig. 1B) the field strength was constant 0.44 T if measured inside the Petri dish. Therefore, this position of the glass plate was preferable for the experiments of contact angle measurements on which 10 or more water droplets were placed in different places.

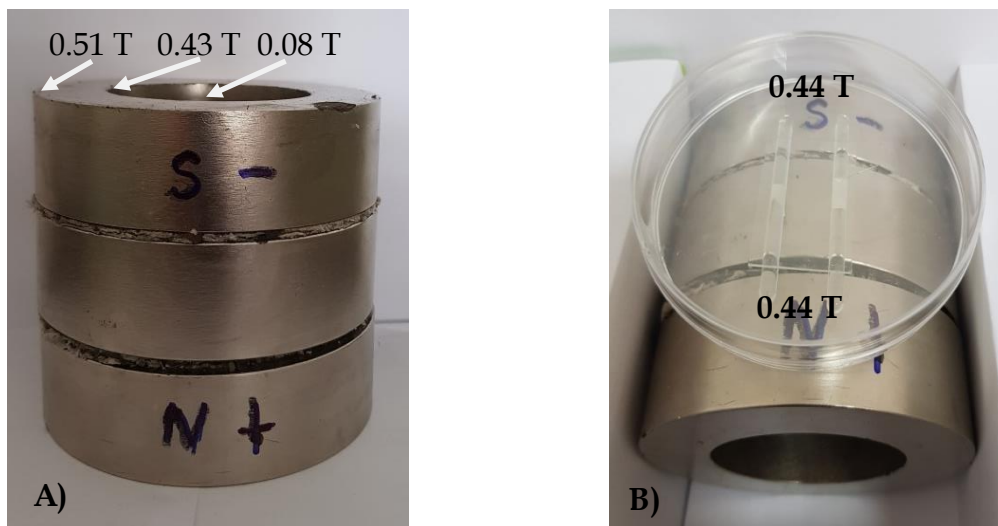


Fig. 1. Setup of neodymium magnet stack with the Petri dish filled with the surfactant solution and the glass plate dipped in it

The plates with the adsorbed surfactant were removed from the solution and placed in a vacuum dryer at  $50^\circ\text{C}$  for 60 min. Next on the plate the advancing and receding contact angles of water were measured.

## 2.5. Contact angle measurements and surface free energy determination

The Digidrop GBX Contact Angle Meter (France) equipped with a video-camera system and computer software was used for the contact angle measurements by the sessile drop method. The advancing contact angles of water (Milli-Q) were measured at  $20 \pm 1^\circ\text{C}$  in a closed chamber after gently settling  $6 \mu\text{l}$  droplets on the surface with a help of automatic deposition system. Then after sucking  $2 \mu\text{l}$  of the solution from the droplet, the receding contact angle was measured. To learn whether the adsorbed layer of the tested surfactants has the same properties if the adsorption occurred from the solution above the glass plate (further called 'top surface') placed in the Petri dish and from the solution below the glass plate (see Fig. 1B), measurements of the advancing and receding water contact angles of water droplets were made on both surfaces of each glass plate, i.e. the 'top' and 'bottom' surfaces of the glass plate. Some small decrease in the magnetic field strength took place across the glass plate thickness which would reflect in the surfactant adsorption. In each system at least 10 advancing and 10 receding contact angles on three plates were measured on both sides of each plate. The following systems were investigated:

- system I: glass/surfactant
- system II: glass/surfactant+MF
- system III: glass-plasma/surfactant
- system IV: glass-plasma/surfactant+MF.

From the mean values of the measured contact angles the apparent surface free energy  $\gamma_s$  was calculated from the equation proposed by Chibowski (Chibowski, 2002; Chibowski and Perea-Cario, 2002; Chibowski, 2003):

$$\gamma_s = \frac{\gamma_l(1+\cos\theta_a)^2}{2+\cos\theta_r+\cos\theta_a} \quad (7)$$

where  $\gamma_l$  is the surface tension of liquid,  $\theta_a$  and  $\theta_r$  are the advancing and receding contact angles, respectively.

## 2.6. Images from the optical profilometer and surface roughness

Using an optical profilometer (Contour GT, Veeco) the images of glass/surfactant surfaces were recorded and the surface roughness by the Wyko Vision software was analyzed. The apparatus is equipped with an optical surface-profiling system (3D) measuring surface morphology with a high accuracy from sub-nanometre up to 10 mm size.

## 3. Results and discussion

Fig. 2 shows the advancing and receding contact angles of water on the DTAB layers adsorbed without (I) and in the presence of a magnetic field (II) on the top and bottom surfaces of non-treated (III) and air-plasma treated glass plates (IV), respectively.

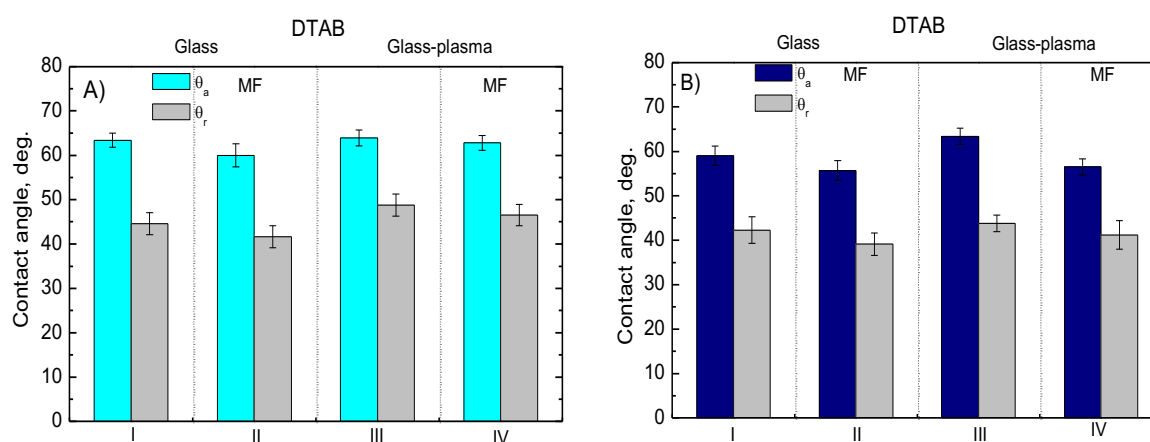


Fig. 2. Advancing and receding contact angles of water on the top (A) and bottom (B) surfaces of glass plates with adsorbed DTAB: I: glass/DTAB; II: glass/DTAB+MF; III: glass-plasma/DTAB; IV: glass-plasma/DTAB+MF

The used concentration of this cationic surfactant ( $10^{-3}$  M) is much below its CMC ( $1.4 \cdot 10^{-2}$  M). As can be seen in the figure a good reproducibility of the results was obtained which is evidenced by the standard deviations of the mean values. In each of the four tested systems, on both sides of the glass plates surface a similar trend of the changes in water contact angles was obtained.

On the bare glass surface  $\theta_a$  is  $34.7 \pm 2.1^\circ$ , while  $\theta_r = 24.1 \pm 1.5^\circ$ , but after the low-temperature air plasma treatment for 60 s, water droplets spread on the surface which indicates that it becomes superhydrophilic (Drelich et al., 2011). Adsorption of DTAB on both glass plates (I: glass/DTAB) and glass plasma treated (III: glass-plasma/DTAB) causes an increase in its hydrophobic properties, as evidenced by the increase in the advancing contact angles to  $63.4 \pm 1.6^\circ$  and  $63.9 \pm 1.8^\circ$  (top surface) and  $59.0 \pm 2.2^\circ$  and  $63.4 \pm 2.2^\circ$  (bottom surface). However, the MF presence during the adsorption caused a small decrease of the contact angles. As already mentioned, the adsorption of DTAB from the  $10^{-3}$  M solution was carried out for 1 h. As the main component of glass is  $\text{SiO}_2$  at the  $\text{pH}=5.7$  its surface has an excess negative charge. At low concentrations the surfactant ions adsorb onto the glass surface via the electrostatic interactions thus neutralizing the surface charge. At the applied concentration the amount of the surfactant ions in the solution may not be sufficient to form the micelles. Therefore, they should adsorb as monomers changing the surface to a more hydrophobic one (Atkin et al., 2003). However, Yi et al. (2018) suggested that on the hydrophilic mica surface at this surfactant concentration a bilayer of the adsorbed molecules may also occur.

Fig. 3 shows similar results plotted for the glass plates with adsorbed CTAB from  $10^{-3}$  M ( $1.06 \times \text{cmc}$ ). The CMC of this surfactant equals  $9.4 \cdot 10^{-4}$  M, hence this concentration is very close to the CMC. As can be seen in this figure the contact angles on the both surfaces (top and bottom) with adsorbed CTAB are

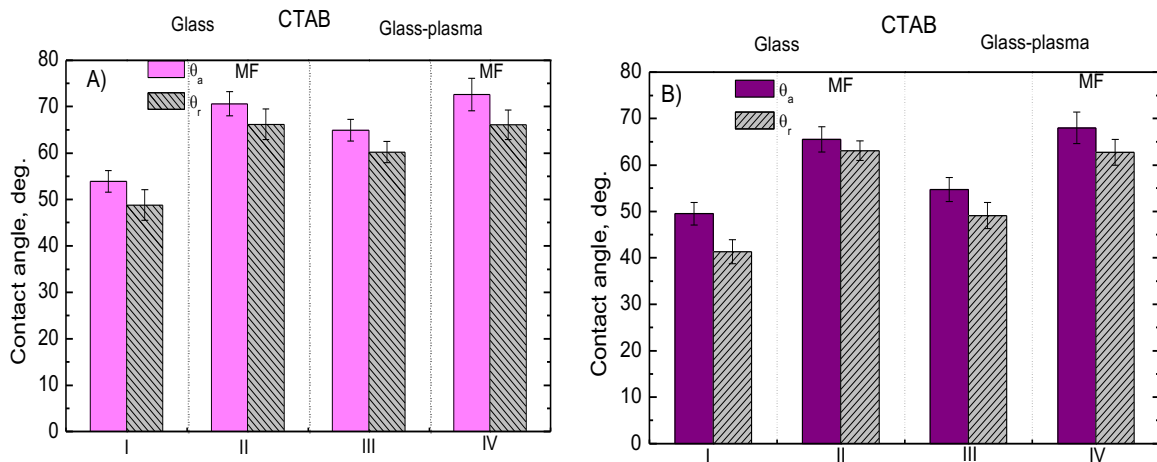


Fig. 3. Advancing and receding contact angles of water on the top (A) and bottom (B) surfaces of glass plates with adsorbed CTAB: I: glass/CTAB; II: glass/CTAB+MF; III: glass-plasma/CTAB; IV: glass-plasma/CTAB+MF

bigger than the value on the bare glass surface ( $\theta_a=34.7\pm 2.1^\circ$ ) and the plasma treatment increases the contact angle. Moreover, contrary to DTAB the MF presence during the adsorption causes a bigger increase of the contact values in comparison to the values measured on the surfaces when the MF field was absent.

In Fig. 4 there are presented the contact angles measured for the analogous systems as above but with  $10^{-3}$  M ( $0.07\times\text{cmc}$ ) anionic SDS. The CMC of this surfactant amounts to  $8.4\cdot 10^{-3}$  M, thus the solution concentration is lower. As it can be clearly seen in the figure, in these systems reproducibility of the contact angle values, which were measured on different places of the plate, both advancing and receding, is very poor which was not the case for CTAB and DTAB (Figs. 2 and 3).

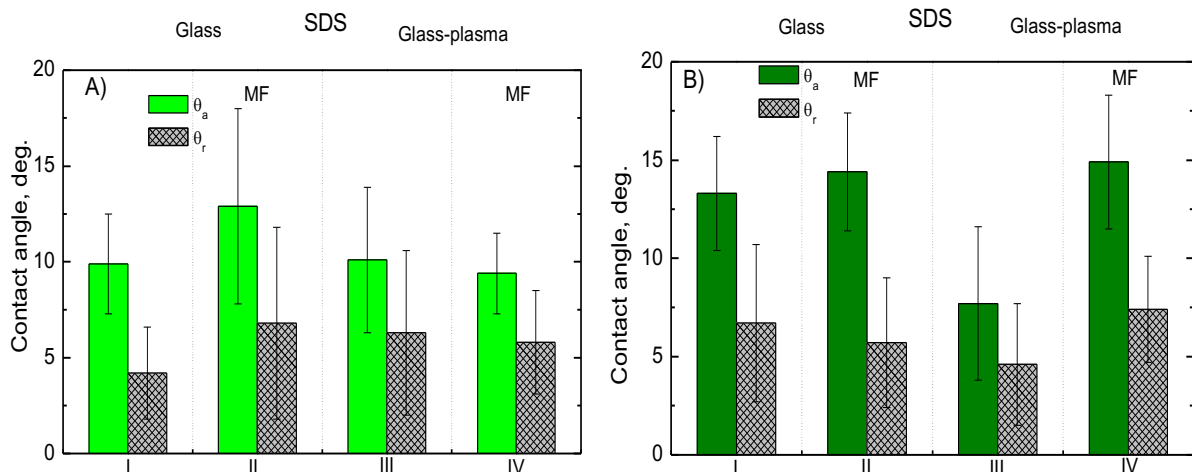


Fig. 4. Advancing and receding contact angles of water on the top (A) and bottom (B) surface of glass plates with adsorbed SDS: I: glass/SDS; II: glass/SDS+MF; III: glass-plasma/SDS; IV: glass-plasma/SDS+MF.

This indicates that the surfaces are not uniformly covered. During the adsorption of a negatively charged head groups of  $\text{DS}^-$  on a negatively charged glass surface hydrophobic interactions and electrostatic repulsion are important. SDS adsorption via hydrophobic interactions occurs between the surfactant tails and the hydrophobic siloxanes on the glass surface (Li and Ishiguro, 2016). Moreover, according to Li and Ishiguro (2016) the negative  $\text{DS}^-$  head group adsorbs on the  $\text{Na}^+$  ion adsorbed layer, and the hydrophobic group of the SDS is directed towards the solution. Then, the hydrophobic carbon chains of the SDS link together by the van der Waals force to form an adsorbed bilayer. Having measured the advancing and receding contact angles, from Eq. (7) the apparent surface free energy  $\gamma_s$  was calculated. The results for all investigated systems are presented in Fig. 5, including those for SDS.

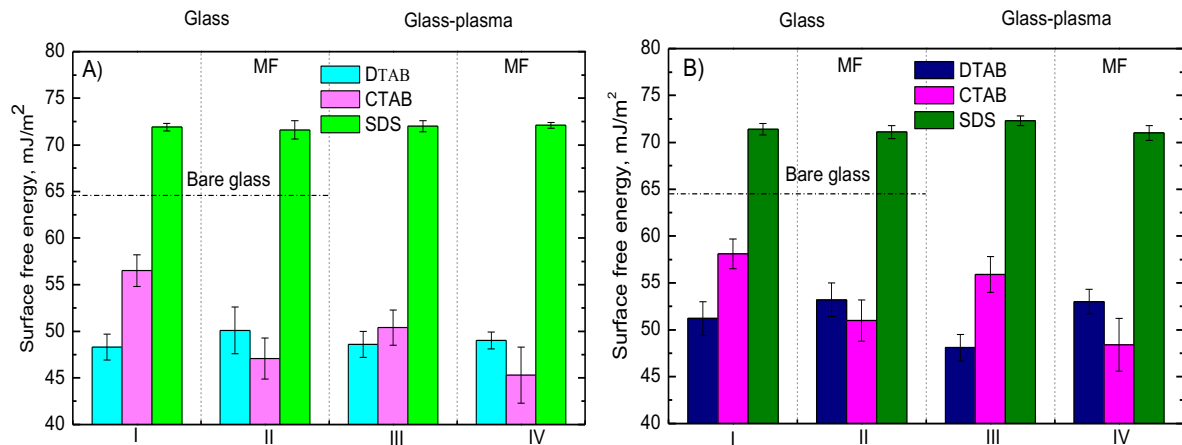


Fig. 5. Surface free energy of adsorbed surfactant layers on the top (A) and bottom (B) surfaces of glass: I: glass/surfactant; II: glass/surfactant+MF; III: glass-plasma/surfactant; IV: glass-plasma/surfactant+MF

The results in Fig. 5 depict changes in the surface hydrophilic/hydrophobic better than the contact angles themselves. Generally, the adsorbed cationic surfactant, DTAB or CTAB, causes a significant decrease in the glass surface free energy. The MF presence causes an increase in the energy if DTAB is used below its CMC and a decrease if CTAB adsorbs in the MF presence, on the top and bottom glass surfaces. A bit greater changes are observed on the bottom surface (B) than on the top one (A). The same is true in the case of DTAB. Moreover, in the case of SDS, although the contact angles are very scattered, using their averaged values it appeared that in all investigated systems the energy is practically the same (Fig. 5) and bigger than that of bare glass surface (64.7 mJm<sup>2</sup>).

To get more information about the structure and topography of the adsorbed layers of the surfactants, images of an optical profilometer were obtained. In the literature the adsorbed layers were investigated with the help of the AFM (Velegol et al, 2000; Xie et al., 2016; Hamon et al, 2018; Yi et al., 2018). However, using AFM technique only images of the layers adsorbed on 1×1 cm<sup>2</sup> size of substrate can be analysed and the tested surface would be too small for the contact angle measurements of a few droplets of a volume 6 μL. Moreover, the tip of AFM apparatus can destroy mechanically the adsorbed layer if in the contact mode. Therefore, for the contact angle measurements we have investigated larger surfaces (3.8×2.6 cm<sup>2</sup> size), and applied optical profilometry techniques the surfaces of 62.5×46.9 μm<sup>2</sup> have been analysed, as well smaller (1.3×0.9 mm<sup>2</sup>) ones. In Table 1 are given values of average roughness  $R_a$  parameters for the all systems studied and the bare and plasma treated glass surfaces.

It appeared that on the glass surface with adsorbed layers of the surfactants one can observed two groups of significantly different values of the parameter  $R_a$ . Therefore in Table 1 there are given the average values for these two groups of  $R_a$ . It means that the surfactants do not adsorb uniformly from the 10<sup>-3</sup> M solutions on the hydrophilic smooth glass surface, which becomes slightly smoother after the plasma treatment. In the case of DTAB on the glass surface there are areas not covered by the surfactant ( $R_a$  values similar as for the bare glass) and surfactant patches with a thickness of 1.9 and 3 nm (bottom and top - III), 4.5 nm (top - I, II and IV, and bottom - II and IV) and 6 nm (bottom - I). Taking into account the DTAB molecule length of 2 nm, it is indicated that only in the III-plasma/DTAB system the surface is not covered by uniform monolayer formed via the electrostatic interactions between the positive charges DTA<sup>+</sup> ions and the oppositely charged the surface sites. The presence of MF influences the adsorption of the bilayer patches which form as a result of the hydrophobic interactions. For the glass/DTAB system no influence of MF on the structure of the adsorbed DTAB layer was observed using this technique.

Yi et al. (2018) studied wettability of adsorbed layers of DTAB on hydrophilic mica by contact angles measurements, the layers morphology and the surface coverage by AFM. When the mica was immersed for 10 min in the solution of DTAB at concentrations of 10<sup>-6</sup> to 10<sup>-3</sup> M the values of advancing contact angle changed from 89.38 to 86.32°. They observed on the mica surface DTAB aggregates in the form of needle-like dots, which at 10<sup>-3</sup> M some of them grow up to flakes. The increase in the concentration from 10<sup>-4</sup> to 10<sup>-3</sup> M at a longer time of adsorption (up to 60 min) caused a decrease of  $\theta_a$  from 89.25 to 73.69

Table 1. Two sets of the mean average height parameter  $R_a$  of bare, plasma treated bare glass surface, and the adsorbed layers of the studied surfactants (top and bottom surfaces of the plates)

System	$R_a$ (1), nm	$R_a$ (2), nm	$R_a$ (1), nm	$R_a$ (2), nm
	Top		Bottom	
Glass	0.59±0.20		0.50±0.21	
Glass-plasma	0.47±0.17		0.37±0.09	
I: Glass/DTAB	0.71±0.23	4.36±0.53	0.69±0.19	5.96±1.29
II: Glass/DTAB+MF	0.60±0.27	4.44±0.53	0.30±0.40	4.54±1.21
III: Glass-plasma/DTAB	0.36±0.05	2.99±0.80	0.34±0.11	1.90±0.20
IV: Glass-plasma/DTAB+MF	0.58±0.23	4.57±0.89	0.30±0.04	4.75±1.81
I: Glass/CTAB	2.06±0.65	3.86±0.26	0.83±0.53	6.60±0.53
II: Glass/CTAB+MF	2.01±0.80	9.01±1.17	0.94±0.37	6.36±1.71
III: Glass-plasma/CTAB	1.58±0.23	3.70±1.25	1.26±0.00	7.64±2.57
IV: Glass-plasma/CTAB+MF	2.52±0.00	6.91±0.97	0.84±0.30	2.56±0.30
I: Glass/SDS	1.52±0.23	3.32±1.26	1.51±0.55	2.73±0.16
II: Glass/SDS+MF	0.76±0.39	2.86±0.67	1.17±0.41	3.20±1.29
III: Glass-plasma/SDS	0.54±0.18	4.76±0.02	0.66±0.57	5.74±0.51
IV: Glass-plasma/SDS+MF	4.40±1.65	13.1±1.29	3.54±0.44	3.54±0.44

as a result of the adsorption of larger aggregates and/or the formation of a bilayer.

In Table 1 it can be seen that in the case of CTAB layers on the top of bare and plasma treated glass surface adsorbed from  $1.06 \times \text{cmc}$  (for  $10^{-3} \text{M}$  solution) without and in the presence of magnetic field: in the system I: Glass/CTAB and III: Glass/CTAB two groups of the surface coverage with the adsorbed surfactant layer were observed, one with a thickness of about 2 nm and the other one with a thickness of about 4 nm. These values are intermediate between the 1 and 2 lengths of  $\text{CTA}^+$  ion which is 2.6 nm (Tanford, 1972). Our results are similar to those of the 3.5 - 4.0 nm layer thickness of CTAB on silica (Velegol et al., 2000) and on quartz (Rennie et al., 1990). This layer thickness is slightly smaller than the diameter of the  $\text{CTAB}^+$  micelles in the solution (4.0-5.0 nm) (Magid, 1998). The AFM study of the CTAB layers adsorbed on silica at  $0.9 \times \text{cmc}$  showed the presence of spheres and short rods ((Velegol et al., 2000). The presence of the magnetic field during CTAB adsorption increases the size of aggregates adsorbed on the bare and plasma treated surface (II: Glass/CTAB+MF and IV: Glass-plasma/CTAB+MF).

Some of the 3D profilometry images for the CTAB adsorbed layers (smaller and larger) are presented in Fig. 6 where the surface roughness parameters:  $R_a$ , root square roughness  $R_q$ , and maximum height of the profile  $R_t$  are also shown.

In the images one can see the above discussed structures of the adsorbed layers which form characteristic aggregates similar to those observed with AFM (Hamon et al., 2018).

Table 1 also shows the changes in the  $R_a$  parameter of SDS layers adsorbed on the glass. In the studied systems (I-IV) at  $10^{-3} \text{M}$  concentration of SDS ( $0.12 \times \text{cmc}$ ) the adsorbed molecules form different size aggregates which appear in the scattered  $R_a$  values. Also the contact angles (Fig. 4) on these surfaces were very poorly reproducible due to the very heterogeneously covered glass surface with the SDS molecules. Shen and Lee (2017) spread  $2 \cdot 10^{-3} \text{M}$  ( $0.22 \times \text{cmc}$  SDS) and  $8.1 \cdot 10^{-3} \text{M}$  ( $1 \times \text{cmc}$ ) solutions on the borosilicate glass and by AFM found stacking aggregates layers of 10, 15, 20 nm at the cmc concentration which formed linear and parallel strips. These results help to understand the scattered values of the parameters obtained by us with the optical profilometer, as well the scattered values of the contact angles obtained on the glass surfaces when the SDS molecules adsorbed from  $10^{-3} \text{M}$  solution.

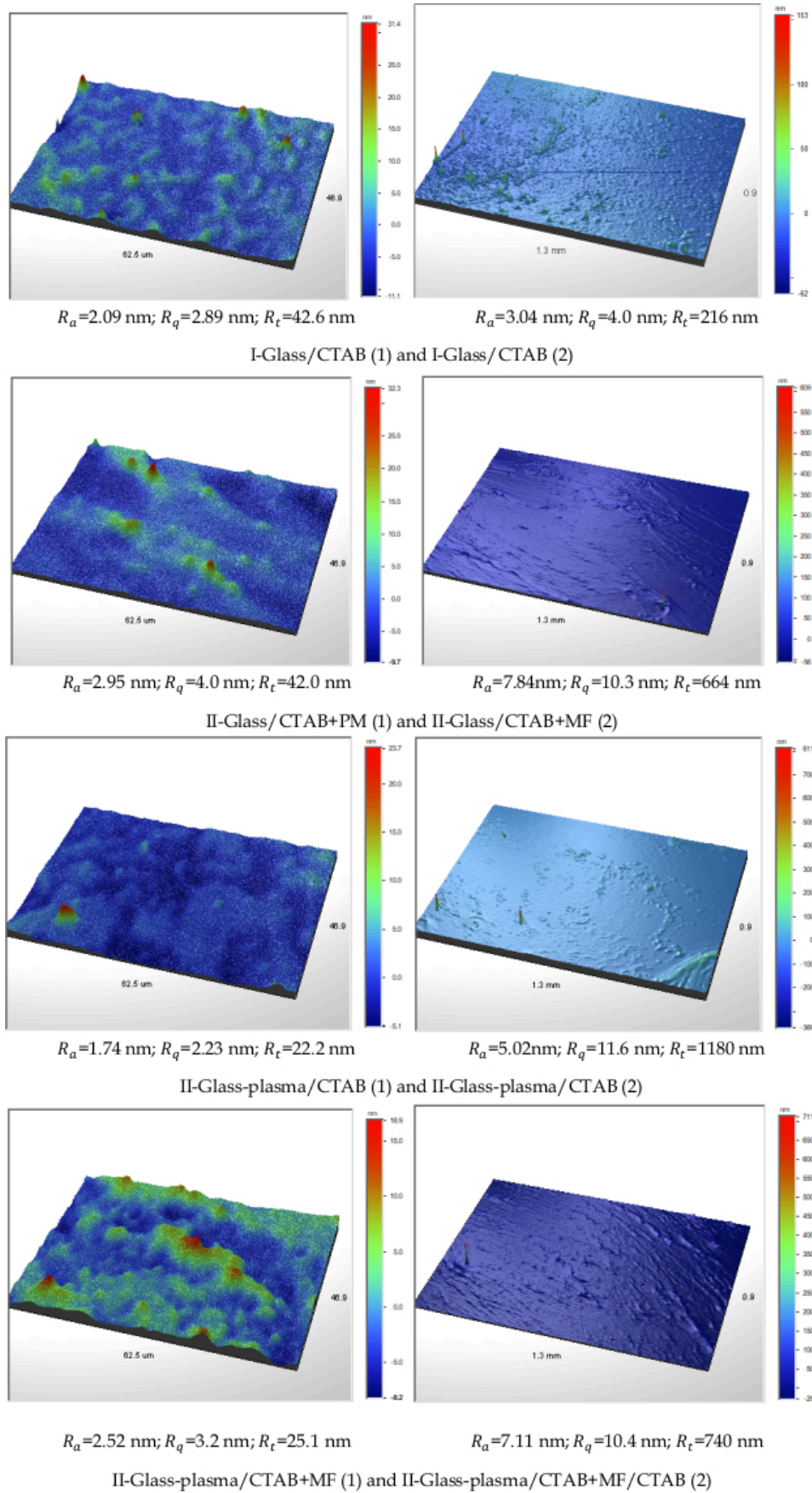


Fig. 6. 3D images of two areas (1 and 2) ( $62.5 \times 46.9 \mu\text{m}^2$  and  $1.3 \times 0.9 \text{ mm}^2$  size) of different thickness of CTAB adsorbed layers on the top of glass plate: I: glass/surfactant; II: glass/surfactant+MF; III: glass-plasma/surfactant; IV: glass-plasma/surfactant+MF with the roughness parameters

#### 4. Conclusions

As was mentioned in the Introduction part, a negative value of the work of water spreading means that water forms a contact angle on the surface. This is a necessary condition for floatation of mineral grains. To depict the changes in the work of spreading  $W_S$  on the investigated surfaces better their values are plotted in Fig. 7.

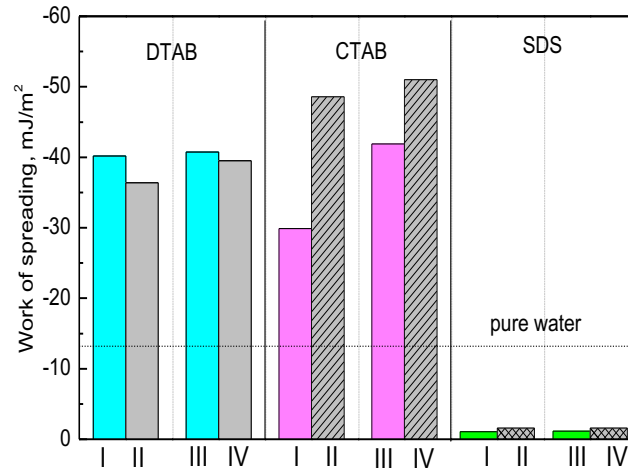


Fig. 7. Changes in the work of water spreading on the investigated surfaces; I: glass/surfactant; II: glass/surfactant+MF; III: glass-plasma/surfactant; IV: glass-plasma/surfactant+MF. The dashed line shows  $W_S$  for pure water. Note: after the plasma treatment water completely spread on the surface

As could be expected, the  $W_S$  values for the cationic surfactants are much more negative than those for pure water on the bare plasma non-treated glass. It means that the surfaces became more hydrophobic than that of the bare glass. In the case of SDS solutions the work of spreading  $W_S$  is evidently less negative than that of pure water on bare glass surface, i.e. the surface is more hydrophilic. The MF presence influences slightly the hydrophilic/hydrophobic property of the surface. The adsorption of the DTAB surfactant in the presence of MF results in a small decrease of the negative work of spreading. However, in the case of CTAB solution the MF caused a distinct increase in the negative work of water spreading. The difference is most probably due to the surfactants concentration below (DTAB) and above (CTAB) critical micelle concentrations and thus to the changes in the structure of the adsorbed layers. In our earlier studies (Chibowski et al., 2019) it was found that MF influence the surface tension of SDS and DTAB solutions which were depended on the concentration. The surface tension of both, anionic and cationic surfactants, was lower after MF treatment. However, below cmc bigger changes were observed for cationic DTAB, and at cmc it increased several mN/m after the treatment. Above the cmc the MF effects were practically vanishing. The observed changes were discussed considering the structure of the surfactant adsorbed layers at the solution/air interface. The Lorentz force acting on the surfactant ions was considered as the driving force. The changes at the solution/air interface should also reflect at solid/solution interface and the structure of the adsorbed layer. But, to propose a detailed mechanism the so far obtained results are not sufficient.

It should be stressed, that we are aware of the fact that these results are preliminary ones and need further verification. However, because of very broad surfactants applications it seems to us that the results can be useful for some practical purposes, not necessarily in the flotation process. More detailed studies will be carried out next.

#### Acknowledgements

We thank to Ms. Patrycja Winiarska for the contact angle measurements.

#### References

ADAMSON, A.W., GAST, A.P., 1997. Physical Chemistry of Surfaces, 5th ed.; New York: Wiley & Sons.

- ALEXANDROVA, L.A., GRIGOROV, L.S., GROZEV, N.A., KARAKASHE, S.I., 2020. *Investigation of interfacial free energy of three-phase contact on a glass sphere in case of cationic-anionic surfactant aqueous mixtures*. *Coatings* 10, 573, 1-14.
- ATKIN, R., CRAIG, V.S.J., WANLESS, E.J., BIGGS, S., 2003. *Mechanism of cationic surfactant adsorption at the solid-aqueous interface*. *Adv. Colloid Interface Sci.* 103, 219-304.
- BAHRI, M.A., HOEBEKE, M., GRAMMENOS, A., DELANAYE, L., VANDESWALLE, N., SERET, A. 2006. *Investigation of SDS, DTAB and CTAB micelle microviscosities by electron spin resonance*. *Colloid Surf. A* 290, 206-212.
- BASTRZYK, A., POLOWCZYK, I., SZELĄG, E., SADOWSKI, Z., 2008. *The effect of protein surfactant interaction on magnesite rock flotation*. *Physicochem. Probl. Miner. Process.* 42, 261-269.
- BÖHMER, M.R., KOOPAL, L.K., 1992a. *Adsorption of ionic surfactants on variable-charge surfaces. 1. Charge effects and structure of the adsorbed layer*. *Langmuir* 8, 2649-2659.
- BÖHMER, M.R., KOOPAL, L.K., 1992b. *Adsorption of ionic surfactants on variable-charge surfaces. 2. molecular architecture and structure of the adsorbed layer*. *Langmuir* 8, 2660-2665.
- CASES, J.M., VILLIERAS, F., 1992. *Thermodynamic model of ionic and nonionic surfactants adsorption-adsorption on heterogeneous surfaces*. *Langmuir* 8, 1251-1264.
- CHIBOWSKI, E., 2002. *Contact angle hysteresis due to a film pressure behind the drop*. *Contact Angle, Wettability and Adhesion*, K.L. Mittal (Ed.), VSP, Utrecht, 265-288.
- CHIBOWSKI, E., PEREA-CARPIO, R., 2002. *Problems of contact angle and solid surface free energy determination*. *Adv. Colloid Interface Sci.* 98, 245-64.
- CHIBOWSKI, E., 2003. *Surface free energy of a solid from contact angle hysteresis*. *Adv. Colloid Interface Sci.* 103, 149-172.
- CHIBOWSKI, E., HOŁYSZ, L., 2006. *Prediction of hydrophobicity/hydrophilicity of a mineral from its surface free energy components in aspect of its flotability*. *Annales Universitatis Mariae Curie-Skłodowska Lublin - Polonia*, LIV/LV8, SECTIO AA, 117-131.
- CHIBOWSKI, E., SZCZEŚ A., HOŁYSZ, L., 2019. *Magnetic field effects on aqueous anionic and cationic surfactant solutions, Part II: Surface tension*, *Edelweiss Chem. Sci. J.* 2, 1-6.
- DIDYK, A.M., SADOWSKI, Z., 2012. *Flotation of serpentinite and quartz using biosurfactants*. *Physicochem. Probl. Miner. Process.* 48(2), 607-618.
- DRELICH, J. W., 2001. *Contact angles measured at mineral surfaces covered with adsorbed collector layer*. *Miner. Metall. Process.* 18(1), 31-37.
- DRELICH, J., CHIBOWSKI, E., MENG, D.D., TERPIŁOWSKI, K., 2011. *Hydrophilic and superhydrophilic surfaces and materials*. *Soft Matter* 7, 9804-9828.
- DRELICH, J. W., 2018. *A simplified analysis of the effect of nano-asperities on particle-bubble interactions*. *Physicochem. Probl. Miner. Process.* 54(1), 10-18.
- DRZYMAŁA, J., 1994. *Hydrophobicity and collectorless flotation of inorganic materials*. *Adv. Colloid Interface Sci.* 50, 143-186.
- DRZYMAŁA, J., 2007. *Mineral processing. Foundations of theory and practice of mineralurgy*. Ofic. Wyd. PWr, Wrocław, Poland.
- DRZYMAŁA, J., SWEBODZIŃSKA, A., DUCHNOWSKA, M., BAKALARZ, A., ŁUSZCZKIEWICZ, A., KOWALCZUK, P.B., 2016. *Preliminary study on collectorless flotation of chalcocite, bornite and copper-bearing shale in the presence of selected frothers*. *Mineral Engineering Conference (MEC 2016), E3S Web of Conferences* 8, 01031. 1-5.
- FAN, A. SOMASUNDARAN, P., TURRO, N.J., 1997. *Adsorption of alkyltrimethylammonium bromides on negatively charged alumina*. *Langmuir* 13, 506-510.
- FUERSTENAU, D.W., HEALY, T.W., SOMASUNDARAN, P. 1964. *The role of the hydrocarbon chain of alkyl collectors in flotation*. *Transactions AIME*, 229, 321-323.
- FUERSTENAU, D.W., SOMASUNDARAN, P., 2003. *Flotation*. In *Principles of Mineral Processing*. ed. M. C. Fuerstenau and K. N. Han. Littleton, CO: Society for Mining, Metallurgy, and Exploration, Inc. (SME), 245-306.
- FUERSTENAU, D.W., JAMESON, G. J., AND YOON R. H., 2007. *Froth Flotation: a Century of Innovation*, SME, Littleton.
- GAO, Y., DU, J. GU, T., 1987. *Hemimicelle formation of cationic surfactants at the silica gel-water interface*. *J. Chem. Soc., Faraday Trans. 1*, 83, 2671-2679.
- GAO, Z., BAL, D., SUN, W., CAO, X., HU, Y., 2015. *Selective flotation of scheelite from calcite and fluorite using a collector mixture*. *Minerals Engineering*. 72, 23-26.

- GAUDIN, A.M., FUERSTENAU, D.W., 1955. *Streaming potential studies. Quartz flotation with cationic collectors* Trans. AIME 202, 958-962.
- GOLOUB, T.P., KOOPAL, L.K., BIJSTERBOSCH, B.H., SIDOROVA, M.P., 1996. *Adsorption of cationic surfactants on silica. surface charge effects.* Langmuir 12(13), 3188-3194.
- GOLOUB, T.P., KOOPAL, L.K., 1997. *Adsorption of cationic surfactants on silica. comparison of experiment and theory.* Langmuir 13(4), 673-681.
- GOLUB, T.P., KOOPAL, L.K., 2004. *Adsorption of cationic surfactants on silica surface: 2. Comparison of theory with experiment.* Colloid J. 66, 44-47.
- GU, T., HUANG, Z., 1989. *Thermodynamics of hemimicellization of cetyltrimethylammonium bromide at the silica gel/water interface.* Colloids Surf. 40, 71-76.
- HARWELL, J.H., HOSKINS, J.C., SCHECHTER, R. S., WADE, W.H., 1985. *Pseudophase separation model for surfactant adsorption: isomerically pure surfactants.* Langmuir 1, 251-262.
- HAMON, J.J., TABOR, R. F. STRIOLO, A., GRADY, B.P., 2018. *Atomic Force Microscopy force mapping analysis of an adsorbed surfactant above and below the critical micelle concentration.* Langmuir 34(25) 7223-7239.
- ISHIGURO, M., KOOPAL, L.K., 2011. *Predictive model of cationic surfactant binding to humic substances.* Colloids Surf. A 379, 70-78.
- LASKOWSKI, J.S., 1989. *Thermodynamic and kinetic flotation criteria.* Miner. Process. Extractive Metall. Rev. 5(1-4), 25-41.
- LEJA, J., 1982. *Surface Chemistry of Froth Flotation.* Plenum Press, NY.
- LI, P., ISHIGURO, M., 2016. *Adsorption of anionic surfactant (sodium dodecyl sulfate) on silica.* Soil Sci. Plant Nutrition 62(3), 223-229.
- LIU, Z., LIAO, Y., AN, M., LAI, Q., MA, L., QIU, Y., 2019. *Enhancing low-rank coal flotation using mixture of dodecane and n-valeraldehyde as a collector.* Physicochem. Probl. Miner. Process. 55(1), 49-57.
- LIU, J-F., MIN, G., DUCKER, W., 2001. *AFM study of adsorption of cationic surfactants and cationic polyelectrolytes at the silica-water interface.* Langmuir 17(16), 4895-4903.
- KARLSSON, P.M., ANDERSON, M.W., PALMQVIST, A.E., 2010. *Adsorption of sodium dodecyl sulfate and sodium dodecyl phosphate at the surface of aluminium oxide studied with AFM.* Corros. Sci. 52, 1103-1105.
- KHAN, A.M., SHAFIQ, F., KHAN, S.A., ALI, S., ISMAIL, B., HAKEEM A.H., RAHDAR, A.M., NAZAR, F., SAYED, M., KHAN, A.R., 2019. *Surface modification of colloidal silica particles using cationic surfactant and the resulting adsorption of dyes.* J. Molec. Liquids 274, 672-680.
- KOOPAL, L.K., GOLOUB, T.P., DAVIS, T.A. 2004. *Binding of ionic surfactants to purified humic acid.* J. Colloid Interface Sci. 275, 360-367.
- KOWALCZUK, P.B., 2015. *Flotation and hydrophobicity of quartz in the presence of hexylamine.* Int. J. Miner. Process. 140, 66-71.
- KOWALCZUK, P.B., ZAWAŁA, J., DRZYMAŁA, J., MAŁYSA, K., 2016. *Influence of hexylamine on kinetics of flotation and bubble attachment to the quartz surface.* Sep. Sci. Technol. 51(15-16), 2681-2690.
- KOWALCZUK, P.B., SIEDLARZ M., SZCZERKOWSKA S., WÓJCIK M., 2017. *Facile determination of foamability index of non-ionic and cationic frothers and its effect on flotation of quartz.* Sep. Sci. Technol. 53(8), 1198-1206.
- MAGID, L.J., 1998. *The surfactant-polyelectrolyte analogy.* J. Phys. Chem. B 102(21), 4064-4074.
- OWENS, D.K., WENDT, R., 1969. *Estimation of the surface free energy of polymers.* J. Appl. Polym. Sci. 13, 1741-174.
- PARIA, S., KHILAR, K.C. 2004. *A review on experimental studies of surfactant adsorption at the hydrophilic solid-water interface.* Adv. Colloid Interface Sci. 110, 75-95.
- RENNIE, A.R., LEE, E M., SIMISTER, E.A., THOMAS, R.K., 1990. *Structure of a cationic surfactant layer at the silica-water interface.* Langmuir 6, 1031-1034.
- Rudolph, M., and Hartman, R., 2017. *Specific surface free energy monponent distributions and flotabilities of mineral microparticles in flotation – An inverse gas chromatography study.* Colloids Surf. A 513, 380-388,
- RUPPRECHT, H., GU, T., 1991. *Structure of adsorption layers of ionic surfactants at the solid/liquid interface.* Colloids Polym. Sci. 269, 506-522.
- SADOWSKI, Z., POLOWCZYK, I., 2004. *Agglomerate flotation on fine oxide particles.* Int. J. Miner. Process. 74, 85-90.
- SCHRAM, L.L., STASIUK, E.N., MARANGONI, D.D., 2003. *Surfactants and their applications.* Annu. Rep. Prog. Chem., Sect. C, 99, 3-48.
- SOKOLOV, I., ZORN, G., NICHOLS, J.M., 2016. *A study of molecular adsorption of a cationic surfactant on complex surfaces with atomic force microscopy.* Analyst 141, 1017-1026.

- SOMASUNDARAN, P., FUERSTENAU, D.W., 1966. *Mechanisms of alkyl sulfonate adsorption at the alumina-water interface*. J. Phys. Chem. 70, 90–96.
- SOMASUNDARAN, P., HUANG, L., 2000. *Adsorption/aggregation of surfactants and their mixtures at solid-liquid interfaces*. Adv. Colloid Interface Sci. 88(1-2), 179–208.
- SZYMAŃSKA, A., SADOWSKI, Z., 2010. *Effects of biosurfactants on surface properties of hematite*. Adsorption 16, 233–239.
- TADMOR, R., DAS, R., GULEC, S., LIU, J. N'GUESSAN, H.E., SHAH, M., WASNIK, P.S., YADAV, S.B., 2017. *Solid-liquid work of adhesion*. Langmuir 33(15) 3594–3600.
- TADMOR, R., BAKSI, A., GULEC, S., JADHAV, S. N'GUESSAN, H.E., SEN, K., SOMASI, V., TADMOR, M., WASNIK, P., YADAV, S., 2019. *Drops that change their mind: spontaneous reversal from spreading to retraction*. Langmuir 35(48), 15734–15738.
- TADMOR, R., BAKSI, A., GULEC, S., JADHAV, S., N'GUESSAN, H.E., SOMASI, V., TADMOR, M., TANG, S., WASNIK, P., YADAV, S., 2020. *Defying gravity: Drops that climb up a vertical wall of their own accord*. J. Colloid Interface Sci. 562, 608–613.
- TADMOR, R., MULTANEN, V., STERN, Y. YAKIR, Y.B., 2021. *Drops retracting while forming a rim*. J. Colloid Interface Sci. 581 Part B, 496–503.
- TANFORD, C.J., 1972. *Micelle shape and size*. Phys. Chem. 76, 3020–3024
- TYRODE, E., RUTLAND, M.W., BAIN, C.D., 2008. *Adsorption of CTAB on hydrophilic silica studied by linear and nonlinear optical spectroscopy*. J. Am. Chem. Soc. 130(51), 17434–17445.
- YESKIE, M.A., HARWELL, J.H., 1988. *On the structure of aggregates of adsorbed surfactants: the surface charge density at the hemimicelle/admicelle transition*. J. Phys. Chem. 92, 2346–2352.
- XIE, Z., JIANG, H., SUN, Z., YANG, Q., 2016. *Direct AFM measurements of morphology and interaction force at solid-liquid interfaces between DTAC/CTAC and mica*. J. Cent. South. Univ. 23, 2182–2190.
- YI, H., ZHANG, X., LU, Y., SONG, S., 2018. *AFM study on the wettability of mica and graphite modified with surfactant DTAB*. J. Dispersion Sci. Technol. 123–126, 213–229.
- VAN OSS, C. J., CHAUDHURY, M. K., AND GOOD, R. J., 1988. *Interfacial Lifshitz-van der Waals and polar interactions in macroscopic systems*. Chem. Rev. 88(6), 927–941.
- ZDZIENNICKA, A., SZYMCZYK, K., KRAWCZYK, J., JAŃCZUK, B., 2012. *Critical micelle concentration of some surfactants and thermodynamic parameters of their micellization*. Fluid Phase Equilibria 322-323, 126–134.
- ZHANG, J., 2013. *Work of adhesion and work of cohesion*. In: Wang Q.J., Chung Y.W. (eds). Encyclopedia of Tribology. Springer, Boston, MA. [https://doi.org/10.1007/978-0-387-92897-5\\_451](https://doi.org/10.1007/978-0-387-92897-5_451)
- ZHANG, R., SOMASUNDARAN, P., 2006. *Advances in adsorption of surfactants and their mixtures at solid/solution interfaces*. Adv. Colloid Interface Sci. 123-126, 213–229.